

### Proton Assisted Oxygen–Oxygen Bond Splitting in Cytochrome P450

André R. Groenhof, Andreas W. Ehlers, and Koop Lammertsma\*

Contribution from the Vrije Universiteit, FEW, Department of Chemistry, De Boelelaan 1083, 1081 HV Amsterdam, The Netherlands

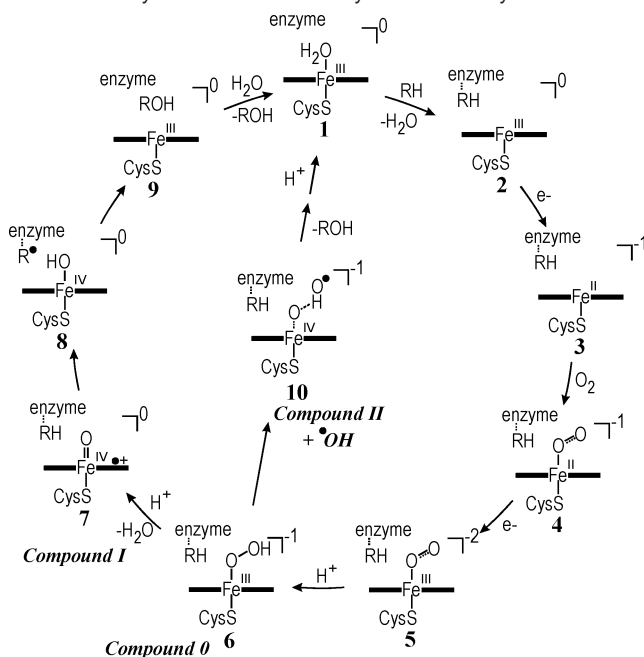
Received November 29, 2006; E-mail: K.Lammertsma@few.vu.nl

**Abstract:** Proton assisted O–O bond splitting of cytochromes' P450 hydroperoxo Compound 0 has been investigated by density functional theory, showing a barrier for the slightly endothermic formation of the iron-oxo Compound I. The barrier and the endothermicity increase with decreasing acidity of the distal proton source. Protonation of the proximal iron heme ligand favors the O–O bond scission and provides an important regulatory component in the catalytic cycle. The Compound 0 → I conversion is slightly exothermic for the peroxidase and catalase models. Implications of the energetic relationship between the two reactive intermediates are discussed in terms of possible oxidative pathways.

#### Introduction

Cytochromes P450 form a ubiquitous family of metabolizing heme-thiolate enzymes that catalyze the monooxygenation of hydrophobic substrates.<sup>1</sup> In this two-electron oxidation one of the oxygen atoms derived from dioxygen inserts, for example, into the C–H bond of a substrate. Most P450 enzymes share similar chemistry, enabling a general description, shown in Scheme 1. It is commonly agreed upon<sup>2–4</sup> that the catalytic cycle starts from the resting state (1) by displacing its axial water ligand for a substrate, followed by iron(III) → iron(II) reduction (2 → 3), oxygen binding (4), a second reduction (4 → 5), and proton transfer to give iron-hydroperoxo 6, known as Compound 0 (Cpd 0), which was recently characterized spectroscopically, be it under cryogenic conditions.<sup>5</sup> The rest of the catalytic cycle is less firmly established. For a long time it has been presumed that 6 leads to iron(IV)oxo porphyrin radical  $\pi$ -cation 7, known as Compound I (Cpd I) and considered to be the active oxidant,<sup>6,7</sup> based on the ability of synthetic models to transfer their oxygen atom to hydrocarbons.<sup>8</sup> While this oxidant has been observed for heme-containing peroxidases and catalases,<sup>9</sup> it

**Scheme 1.** Cytochrome P450 Catalytic Reaction Cycle<sup>a</sup>



<sup>a</sup> RH represents the substrate; ROH, the product; and –Fe–, the iron protoporphyrin IX.

remains elusive for the P450s.<sup>1a,10</sup> There is a growing consensus that the oxidative mechanism may be more complex than hitherto assumed, and recently this has been formulated in the

- (1) (a) Ortiz de Montellano, P. R., Ed. *Cytochrome P450: Structure, Mechanism and Biochemistry*, 3rd ed; Kluwer Academic/Plenum Publishers: New York, 2005. (b) Denisov, I. G.; Markis, T. M.; Sligar, S. G.; Schlichting, I. *Chem. Rev.* **2005**, *105*, 2253–2278. (c) Sono, M.; Roach, M. P.; Coulter, E. D.; Dawson, J. H. *Chem. Rev.* **1996**, *96*, 2841–2888.
- (2) Mueller, E. J.; Loida, P. J.; Sligar, S. G. In *Cytochrome P450: Structure, Mechanism and Biochemistry*, 2nd ed.; Ortiz de Montellano, P. R., Ed.; Plenum Press: New York, 1995; pp 83–124.
- (3) Shaik, S.; Kumar, D.; De Visser, S. P.; Altun, A.; Thiel, W. *Chem. Rev.* **2005**, *105*, 2279–2328. (b) Meunier, B.; De Visser, S. P.; Shaik, S. *Chem. Rev.* **2004**, *104*, 3947–3980. (c) Loew, G. H.; Harris, D. J. *Chem. Rev.* **2000**, *100*, 407–419.
- (4) Rydberg, P.; Sigfridsson, E.; Ryde, U. *J. Biol. Inorg. Chem.* **2004**, *9*, 203–223.
- (5) (a) Schlichting, I.; Berendzen, J.; Chu, K.; Stock, A. M.; Maves, S. A.; Benson, D. E.; Sweet, R. M.; Ringe, D.; Petsko, G. A.; Sligar, S. G. *Science* **2000**, *287*, 1615–1622. (b) Davydov, R.; Makris, T. M.; Kofman, V.; Werst, D. E.; Sligar, S. G.; Hoffman, B. M. *J. Am. Chem. Soc.* **2001**, *123*, 1403–1415.
- (6) (a) Groves, J. T.; McClusky, G. A. *J. Am. Chem. Soc.* **1976**, *98*, 859–861. (b) Groves, J. T.; McClusky, G. A.; White, R. E.; Coon, M. J. *Biochem. Biophys. Res. Commun.* **1978**, *81*, 154–160.

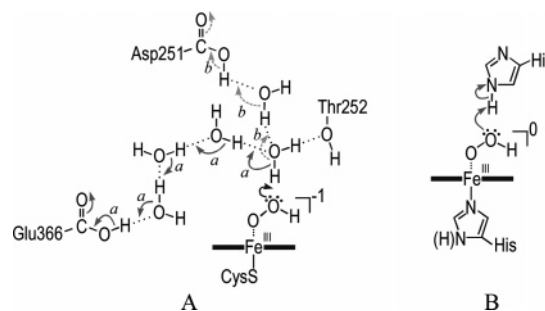
- (7) (a) Schöneboom, J. C.; Cohen, S.; Lin, H.; Shaik, S.; Thiel, W. *J. Am. Chem. Soc.* **2004**, *126*, 4017–4034. (b) Schöneboom, J. C.; Lin, H.; Reuter, N.; Thiel, W.; Cohen, S.; Ogliaro, F.; Shaik, S. *J. Am. Chem. Soc.* **2002**, *124*, 8142–8151. (c) Ogliaro, F.; De Visser, S. P.; Cohen, S.; Kaneti, J.; Shaik, S. *ChemBioChem* **2001**, *11*, 848–851. (d) Ogliaro, F.; Harris, N.; Cohen, S.; Filatov, M.; De Visser, S. P.; Shaik, S. *J. Am. Chem. Soc.* **2000**, *122*, 8977–8989.
- (8) Groves, J. T.; Haushalter, R. C.; Nakamura, M.; Nemo, T. E.; Evans, B. J. *J. Am. Chem. Soc.* **1981**, *103*, 2884–2886.

two-state versus multiple oxidant models.<sup>11–14</sup> For example, current theoretical studies indicate the oxygen rebound mechanism of Cpd I with substrates to possibly involve both the doublet and quartet states.<sup>3</sup> We also note that Cpd 0 is thought to be the active oxidant for enzyme mutants wherein its lifetime is prolonged<sup>13</sup> and for the conversion of heme to biliverdin by heme oxygenase.<sup>15</sup> Further, two alkane hydroxylation pathways were recently described that are energetically (nearly) competitive with the Cpd I route, but which start with a different cleavage of the oxygen–oxygen bond of Cpd 0. In both a hydroxyl radical is formed, H-bonded to the anionic metal oxide ( $-\text{FeO}\cdots\text{HO}\bullet$ , Cpd II), that converts to water on abstraction of a hydrogen atom from the alkane.<sup>12</sup> They differ in that the subsequent hydroxylation step involves either a concerted hydrogen atom transfer of this water molecule with a concomitant rebound of the carbon radical to the incipient hydroxyl radical<sup>12b</sup> or a direct rebound to the oxygen atom of Cpd II.<sup>12a</sup>

Depending on the alkane and the theoretical method that is used, the estimate for the activation energy for the homolytic O–O bond cleavage for the Cpd 0  $\rightarrow$  II conversion ranges from 19.4 to 24.8 kcal mol<sup>-1</sup>,<sup>12</sup> and that for the rate-determining H-abstraction from the alkane in the Cpd I oxygen rebound process ranges from 14.0 to 28.6 kcal mol<sup>-1</sup>.<sup>7,16</sup> If these two routes are to present competing oxidation channels, as the similarity in reaction barriers (using similar levels of theory) might suggest, then it is critically important to carefully calibrate the relationship between Cpd 0 and I, which is the intent of the present study.

The Cpd 0  $\rightarrow$  I conversion likely occurs by protonating the outer oxygen atom,<sup>17</sup> implying that acid–base chemistry underlies the dioxygen bond scission. However, the P450s have no strategically positioned acid–base catalyst for dioxygen to be protonated such as the histidine amino acid residue in peroxidases and catalases<sup>18–20</sup> or the glutamic acid in chloro

**Scheme 2.** Proton Delivery Models for (A) P450cam and (B) Peroxidases



peroxidases<sup>21,22</sup> for which Cpd I has been determined experimentally. Instead, a conserved acid–alcohol pair is speculated to enable the protonation of P450s' Cpd 0.<sup>17</sup> In the case of P450cam (CYP101), aspartic acid D251 or glutamic acid E366 and threonine residue T252 are presumably part of a complex hydrogen-bonded network that enables proton delivery (Scheme 2A),<sup>5a,23</sup> which then depends on the protein conformation and on the local pH. The site of protonation and the conditions for releasing a water molecule are thus critical for generating Cpd I, for which its properties have been studied by theoretical methods in far greater detail<sup>7,16,24</sup> than the manner in which it may be formed.<sup>25c,d</sup> Using a bare proton reportedly gives a highly exothermic reaction (about  $-330$  kcal mol<sup>-1</sup>) without barrier,<sup>25</sup> resulting in the assumption that water is released spontaneously to form Cpd I. This assumption contrasts with the fact that Cpd 0 is sufficiently long-lived to be observed at low temperature, while Cpd I is not.<sup>1,5</sup> The exothermicity of the O–O bond scission reduces from  $-330$  to  $-158.6$  kcal mol<sup>-1</sup> when the hydronium ion is the protonating agent and becomes even endothermic by  $+64.2$  kcal mol<sup>-1</sup> when neutral water is used.<sup>25c</sup> These large energy differences reflect the dominance of electrostatic effects in the gas-phase calculations. Proton transfer from threonine via an intervening water molecule reportedly gives a more realistic exothermicity of only  $-5.5$  kcal mol<sup>-1</sup>, which contrasts, however, strongly with the  $-80$  kcal mol<sup>-1</sup> obtained in a QM/MM study.<sup>24b,25a,26</sup> During the course of the present study, Shaik and co-workers<sup>11</sup> found, using geometry scans, similar energies for Cpd 0 and I, suggesting that a barrier exists for the interconversion. In summary, it appears that there is no consensus concerning the relative

- (9) (a) Rutter, R.; Hager, L. P.; Dhonau, H.; Hendrich, M.; Valentine, M.; Debrunner, P. *Biochemistry* **1984**, *23*, 6809–6816. (b) Berglund, G. I.; Carlsson, G. H.; Smith, A. T.; Szöke, H.; Hendriksen, A.; Hajdu, J. *Nature* **2002**, *417*, 463–468.
- (10) White, R. E.; Coon, M. J. *Annu. Rev. Biochem.* **1980**, *49*, 315–356.
- (11) Kumar, D.; Hirao, H.; De Visser, S. P.; Zheng, J.; Wang, D.; Thiel, W.; Shaik, S. *J. Phys. Chem. B* **2005**, *109*, 19946–19951.
- (12) (a) Derat, E.; Kumar, D.; Hirao, H.; Shaik, S. *J. Am. Chem. Soc.* **2006**, *128*, 473–484. (b) Bach, R. D.; Dmitrenko, O. *J. Am. Chem. Soc.* **2006**, *128*, 1474–1488.
- (13) (a) Ortiz de Montellano, P. R.; De Voss, J. *J. Nat. Prod. Rep.* **2002**, *19*, 477–493. (b) Chandrasena, R. E. P.; Vatsis, K. P.; Coon, M. J.; Hollenberg, P. F.; Newcomb, M. *J. Am. Chem. Soc.* **2004**, *126*, 115–126. (c) Newcomb, M.; Aebischer, D.; Shen, R.; Chandrasena, R. E. P.; Hollenberg, P. F.; Coon, M. J. *J. Am. Chem. Soc.* **2003**, *125*, 6064–6065. (d) Newcomb, M.; Chandrasena, R. E. P. *Biochem. Biophys. Res. Commun.* **2005**, *338*, 394–403. (e) Raag, R.; Martinis, S. A.; Sliagar, S. G.; Poulos, T. L. *Biochemistry* **1991**, *30*, 11420–11429. (f) Newcomb, M.; Shen, R.; Choi, S. Y.; Toy, P. H.; Hollenberg, P. F.; Vaz, A. D. N.; Coon, M. J. *J. Am. Chem. Soc.* **2000**, *122*, 2677–2686. (g) Davydov, R.; Perera, R.; Jin, S.; Yang, T.-C.; Bryson, T. A.; Sono, M.; Dawson, J. H.; Hoffman, B. M. *J. Am. Chem. Soc.* **2005**, *127*, 1403–1413.
- (14) (a) Jin, S.; Bryson, T. A.; Dawson, J. H. *J. Biol. Inorg. Chem.* **2004**, *9*, 644–653. (b) Nam, W.; Ryu, Y. O.; Song, W. *J. Biol. Inorg. Chem.* **2004**, *9*, 654–660. (c) Shaik, S.; De Visser, S. P.; Kumar, D. *J. Biol. Inorg. Chem.* **2004**, *9*, 661–668. (d) Newcomb, M.; Hollenberg, P. F.; Coon, M. J. *Arch. Biochem. Biophys.* **2003**, *409*, 72–79.
- (15) Matsui, T.; Kim, S. H.; Jin, H.; Hoffman, B. M.; Ikeda-Saito, M. *J. Am. Chem. Soc.* **2006**, *128*, 1090–1091.
- (16) (a) De Visser, S. P.; Kumar, D.; Cohen, S.; Shacham, R.; Shaik, S. *J. Am. Chem. Soc.* **2004**, *126*, 8362–8363. (b) Ogliaro, F.; Filatov, M.; Shaik, S. *Eur. J. Inorg. Chem.* **2000**, 2455–2458. (c) Yoshizawa, K.; Kagawa, Y.; Shiota, Y. *J. Phys. Chem. B* **2000**, *104*, 12365–12370.
- (17) Makris, T. M.; Denisov, I.; Schlichting, I.; Sliagar, S. G. In *Cytochrome P450: Structure, Mechanism and Biochemistry*, 3rd ed.; Ortiz de Montellano, P. R., Ed.; Kluwer Academic/Plenum Publishers: New York, 2005; pp 149–182.
- (18) Poulos, T. L.; Finzel, B. In *Peptide and Protein Reviews*; Heran, M. T. W., Ed.; Marcel Dekker: New York, 1984; pp 115–171.

- (19) Poulos, T. L.; Kraut, J. *J. Biol. Chem.* **1980**, *255*, 8199–8205.
- (20) Maté, M. J.; Murshudov, G.; Bravo, J.; Melik-Adamyany, W.; Loewen, P. C.; Fita, I. In *Handbook of Metalloproteins*; Messerschmidt, A., Huber, R., Poulos, T., Wieghardt, K., Eds.; Wiley: Chichester, 2001; pp 486–502.
- (21) Sundaramoorthy, M. In *Handbook of Metalloproteins*; Messerschmidt, A., Huber, R., Poulos, T., Wieghardt, K., Eds.; Wiley: Chichester, 2001; pp 233–244.
- (22) Stone, K. L.; Behan, R. K.; Green, M. T. *Proc. Natl. Acad. Sci. U.S.A.* **2005**, *102*, 16563–16565.
- (23) (a) Vidakovic, M.; Sliagar, S. G.; Li, H.; Poulos, T. L. *Biochemistry* **1998**, *37*, 9211–9219. (b) Aikens, J.; Sliagar, S. G. *J. Am. Chem. Soc.* **1994**, *116*, 1143–1144. (c) Gerber, N. C.; Sliagar, S. G. *J. Biol. Chem.* **1994**, *269*, 4260–4266. (d) Taraphder, S.; Hummer, G. *J. Am. Chem. Soc.* **2003**, *125*, 3931–3940.
- (24) (a) Schöneboom, J. C.; Neese, F.; Thiel, W. *J. Am. Chem. Soc.* **2005**, *127*, 5840–5853. (b) Kamachi, T.; Yoshizawa, K. *J. Am. Chem. Soc.* **2003**, *125*, 4652–4661. (c) Harris, D.; Loew, G.; Waskell, L. *J. Inorg. Biochem.* **2001**, *83*, 309–318. (d) Ogliaro, F.; Cohen, S.; De Visser, S. P.; Shaik, S. *J. Am. Chem. Soc.* **2000**, *122*, 12892–12893. (e) Filatov, M.; Harris, N.; Shaik, S. *J. Chem. Soc., Perkin Trans. 2* **1999**, 399–410.
- (25) (a) Guallar, V.; Friesner, R. A. *J. Am. Chem. Soc.* **2004**, *126*, 8501–8508. (b) Guallar, V.; Harris, D. L.; Bastista, V. S.; Miller, W. H. *J. Am. Chem. Soc.* **2002**, *124*, 1430–1437. (c) Ogliaro, F.; De Visser, S. P.; Shaik, S. *J. Inorg. Biochem.* **2002**, *91*, 554–567. (d) Harris, D. J.; Loew, G. H. *J. Am. Chem. Soc.* **1998**, *120*, 8941–8948.

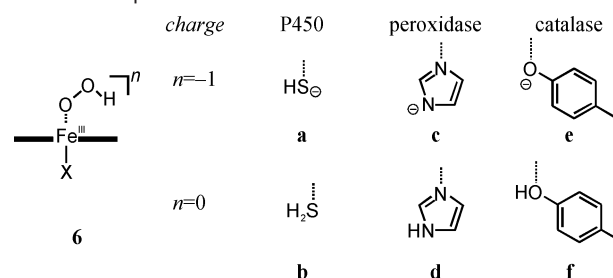
energies of Cpd 0 and Cpd I. To enhance the insight into the catalytic cycle, as either one of the reactive intermediates could be the kinetically active oxidant for alkane hydroxylation,<sup>14,27</sup> we evaluate in detail the energetic relationship between Cpd 0 and I using density functional theory (DFT) for model structures. The GGA exchange functional OPTX<sup>28</sup> in combination with the PBE<sup>29</sup> correlation functional (OPBE) is used because of its demonstrated superior performance (spin states, electronic structures) for iron complexes.<sup>30,31</sup>

### Computational Details

Calculations were performed with the Amsterdam Density Functional (ADF) program.<sup>32</sup> The atomic orbitals on all atoms were described by an uncontracted triple- $\zeta$  valence plus polarization STO basis set (TZP). The inner cores of carbon, nitrogen, and oxygen ( $1s^2$ ) and those of sulfur and iron ( $1s^2 2s^2 2p^6$ ) were kept frozen.<sup>32a,33</sup> The exchange-correlation potential is based on the newly developed GGA exchange functional OPTX<sup>28</sup> in combination with the nonempirical PBE<sup>29</sup> for correlation (OPBE). The Farkas similar weighted combination of the BFGS and SR1 schemes is used for updating the Hessian in the geometry optimizations. In calculating the potential energy surface (PES, Figure 2) a DZP basis set was used for the porphyrin periphery carbon and hydrogen atoms, whereas all other atoms were described by a TZP basis set. The vibrational eigenvectors associated with the imaginary frequency of all the transition states were analyzed to confirm their connectivity with the reactants and products; no IRC calculations were performed.

In addition, the energy difference between Cpd 0 and Cpd I was also investigated at the QM/MM level. These calculations were performed using a recent implementation within ADF using the AMBER95<sup>34</sup> force field for describing the interactions within the protein environment and those of the QM atoms with the MM atoms. The QM/MM boundaries were treated by using the AddRemove coupling scheme developed by Swart.<sup>35</sup> The QM/MM model used the geometry of the crystal structure of the cytochrome P450cam (1DZ8)<sup>5a</sup> as the starting structure and consists of 7580 atoms. The QM subsystem consists of the heme (without the full propionate side chains), the side chains of Cys357 and Glu366, and four crystal water molecules W523, W566, W902, and W901. The covalent bonds cut at the QM/MM border are saturated by hydrogen link atoms, giving a QM subsystem of 125 atoms that was treated at the DFT level as described above. The reported energies refer to QM energies computed in the presence of the MM point charges. See Supporting Information for more details.

### Scheme 3. Cpd 0 Models<sup>a</sup>



<sup>a</sup> Thiolate (a) and sulfide (b) mimic the cysteine ligand in P450s; imidazolate (c) and imidazole (d) mimic the histidine ligand in peroxidases; and 4-methyl phenolate (e) and 4-methyl phenol (f) mimic the tyrosine ligand in catalases.

**Table 1.** Relative Energies (kcal·mol<sup>-1</sup>) of the Electronic States of Cpd 0 (6) with Different Axial Ligands<sup>a</sup>

axial ligand		spin state		
		doublet	quartet	sextet
HS <sup>-</sup>	<b>6a</b>	0.0 (0.81)	15.0 (3.86)	13.8 (8.87)
Im <sup>-</sup>	<b>6c</b>	0.0 (0.79)	17.2 (3.85)	13.6 (8.84)
MePhO <sup>-</sup>	<b>6e</b>	0.0 (0.81)	12.3 (3.87)	6.8 (8.83)

<sup>a</sup> Values in parentheses refer to computed  $S^2$  values (for pure spin states the values are 0.75 (doublet), 3.75, (quartet), and 8.75 (sextet)).

### Results and Discussion

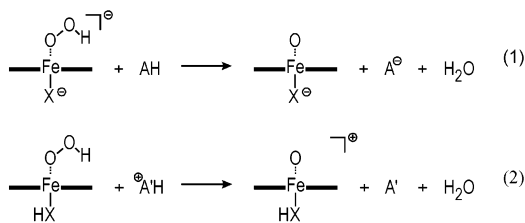
Cleaving the O–O bond in hydroperoxo Cpd 0 (6) is a crucial mechanistic step in the catalytic cycle of heme containing oxygenating enzymes that include cytochromes P450, peroxidases, and catalases. Presumably Cpd I is formed on protonating the outer oxygen atom of Cpd 0. We investigated this reaction for the hydroperoxo iron porphyrin species bearing a thiolate (6a), imidazolate (6c), and a 4-methylphenolate (6e) proximal ligand to mimic the cysteine, histidine, and tyrosine moieties in the active site of P450s, peroxidases, and catalases, respectively (Scheme 3). The charge of these ligands is  $-1$ , which may, however, be neutralized by second sphere amino acid interactions and by the local pH in the proximal region.<sup>20,36,37</sup> Hence, because neutral ligands are feasible for peroxidases and catalases and for the sake of completeness, we also include in this study neutral ligands, i.e., 6b,d,f (Scheme 3).

Cpd 0 can exist in a doublet, quartet, or sextet state, with respectively one, three, and five unpaired electrons. The active site models were optimized for each spin state. The relative energies for the anionic ligands (Table 1) show that in all cases the doublet state is the lowest in energy. The doublet/sextet energy gap of the 4-methyl phenolate model is about half that of the other two ligands due to stabilization of the high spin state by a larger contribution of the XC energy, probably caused by reduced repulsion of electrons with different spins. The doublet state is the only viable one when Cpd 0 carries an uncharged proximal ligand (6b,d,f) as the quartet and sextet states were found to be dissociative for the proximal ligand.<sup>38</sup> Hence, we focus on the doublet spin state only in evaluating the protonation and oxygen–oxygen bond scission process.

To describe the (gas phase) protonation that leads to Cpd I, charge separation and recombination must be avoided to prevent the otherwise dominant electrostatic effects. Therefore, un-

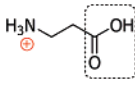
- (26) A surprisingly large exothermicity of  $-80$  kcal mol<sup>-1</sup> was reported in a QM/MM study<sup>25a</sup> that contrasts with our results using a similar methodology (vide infra). It has been recognized, however, that the optimization protocol and choices of the starting structure are of critical importance for energy evaluations as shown, for example, for the hydrogen abstraction and oxygen rebound steps; see: (a) Altun, A.; Shaik, S.; Thiel, W. *J. Comput. Chem.* **2006**, *27*, 1324. (b) Altun, A.; Guallar, V.; Friesner, R. A.; Shaik, S.; Thiel, W. *J. Am. Chem. Soc.* **2006**, *128*, 3924.
- (27) Coon, M. J. *Biochem. Biophys. Res. Commun.* **2003**, *312*, 163–168.
- (28) Handy, N. C.; Cohen, A. J. *Mol. Phys.* **2001**, *99*, 403–412.
- (29) Perdew, J. P.; Burke, K.; Ernzerhof, M. *Phys. Rev. Lett.* **1996**, *77*, 3865–3868.
- (30) Swart, M.; Groenhof, A. R.; Ehlers, A. W.; Lammertsma, K. *J. Phys. Chem. A* **2004**, *108*, 5479–5483.
- (31) Groenhof, A. R.; Swart, M.; Ehlers, A. W.; Lammertsma, K. *J. Phys. Chem. A* **2005**, *109*, 3411–3417.
- (32) (a) Te Velde, G.; Bickelhaupt, F. M.; Van Gisbergen, S. J. A.; Fonseca Guerra, C.; Baerends, E. J.; Snijders, J. G.; Ziegler, T. *J. Comput. Chem.* **2001**, *22*, 931–967. (b) Fonseca Guerra, C.; Snijders, J. G.; Te Velde, G.; Baerends, E. J. *Theor. Chem. Acc.* **1988**, *99*, 391–403. (c) ADF2005.01, SCM, Theoretical Chemistry, Vrije Universiteit: Amsterdam, The Netherlands; <http://www.scm.com>.
- (33) (a) Baerends, E. J.; Ellis, D. E.; Ros, P. *Theor. Chim. Acta* **1972**, *27*, 339–354.
- (34) Cornell, W. D.; Cieplak, P.; Bayly, C. I.; Gould, I. R.; Merz, K. M., Jr.; Ferguson, D. M.; Spellmeyer, D. C.; Fox, T.; Caldwell, J. W.; Kollman, P. A. *J. Am. Chem. Soc.* **1995**, *117*, 5179–5197.
- (35) Swart, M. *Int. J. Quantum Chem.* **2002**, *91*, 177–183.

- (36) Perera, R.; Sono, S.; Sigmandagger, J. A.; Pfisterdagger, T. D.; Ludagger, Y.; Dawson, J. H. *Proc. Natl. Acad. Sci. U.S.A.* **2003**, *100*, 3641–3646.
- (37) Derat, E.; Cohen, S.; Shaik, S.; Altun, A.; Thiel, W. *J. Am. Chem. Soc.* **2005**, *127*, 13611–13621.

**Scheme 4.** Cpd I Formation Model Reactions Starting with Either an Anionic (eq 1) or a Neutral (eq 2) Cpd 0 Species**Table 2.** Cpd 0 → I Reaction Energies (kcal·mol<sup>-1</sup>) with ZPE Correction Values in Parentheses for P450 (HS<sup>-</sup>), Peroxidase (Im<sup>-</sup>), and Catalase (MePhO<sup>-</sup>) Models Using Model Reaction 1 (See Scheme 4)

proton source AH (pK <sub>a</sub> )	(heme protein) proximal ligand X		
	(P450) HS <sup>-</sup> (6a)	(peroxidase) Im <sup>-</sup> (6c)	(catalase) MePhO <sup>-</sup> (6e)
formic acid (3.8)	3.6 (0.3)	9.8 (6.2)	-0.9 (-4.5)
3-aminopropanoic acid β-alanine (3.6)	5.8 (2.4)	12.0 (8.3)	1.3 (-2.3)
imidazole (14.5)	9.3 (5.8)	15.5 (11.7)	4.8 (1.1)
isopropanol (17.1)	35.2 (30.7)	41.5 (36.6)	30.7 (25.9)

**Table 3.** Compound 0 → Compound I Reaction Energies (kcal·mol<sup>-1</sup>) with ZPE Correction Values in Parentheses for P450 (H<sub>2</sub>S), Peroxidase (ImH), and Catalase (MePhOH<sup>⊕</sup>) Models Using Model Reaction 2 (See Scheme 4)

Proton source A'H <sup>+</sup> (pK <sub>a</sub> )	(heme protein) proximal ligand HX		
	(P450) H <sub>2</sub> S	(peroxidase) ImH	(catalase) MePhOH <sup>⊕</sup> [ <sup>a</sup> ]
hydronium ion	-93.6	-99.4	[-97.9]
 3-aminopropanoic acid β-alanine-H <sup>+</sup>	2.3 (-3.6)	-3.4 (-9.0)	[-1.9] [(-7.2)]

<sup>a</sup> The phenolate oxygen–iron bond is frozen in the optimizations.<sup>38</sup>

charged acids should be used for anionic Cpd 0 (**6a,c,e**; *model reaction 1*), and cationic ones, for uncharged Cpd 0 (**6b,d,f**; *model reaction 2*) (Scheme 4). Yet, as noted, strong acids like the hydronium ion give improbably large exothermicities for the protein mediated protonations (Table 3), underscoring that moderate acids should be used instead. Moreover, to compare model reactions 1 and 2 with each other the same ultimate proton donor should be applied, which can be accomplished by using a zwitterion. Thus, the carboxylic acid group of 3-aminopropanoic acid (β-alanine) is used as a proton donor with the amino moiety serving to differentiate between the neutral (Table 2) and protonated acid (Table 3). The involvement of a carboxylic acid side chain in the P450 proton machinery forms another reason for using β-alanine as a proton donor mimic in these QM calculations (Scheme 2A).<sup>17</sup> In model reaction 1, three additional proton donors, i.e., formic acid, imidazole, and isopropanol, are used to study the influence of the acid strength

(38) Optimizations of both the 4-methyl phenol Compound 0 (**6f**) and Compound I (**7f**) species as isolated molecules (gas phase) result in cleavage of the phenolate oxygen–iron bond. This may indicate a critical role of the surrounding polar pocket for the protonation of the phenolate. In the present study, **6f** and **7f** are fully optimized while restraining their phenolate oxygen–iron bonds to 2.287 and 2.602 Å, respectively. These bond distances were estimated from the optimized structures (**6** and **7**) with 4-methyl phenolate coordinated to methyl-guanidinium as an axial ligand to mimic the tyrosine/arginine pair in catalases.

(local pH). Formic acid and isopropanol mimic glutamic (or aspartic) acid and threonine that are present in the P450 active site (Scheme 2A) and imidazole as the histidine in peroxidases and catalases (Scheme 2B). For these acids, the OPBE/TZP calculated (gas phase, 298 K) proton affinities of the conjugate bases are in excellent agreement with experimentally determined values with a mean deviation of only 1.3 kcal mol<sup>-1</sup> (Table S1), thereby validating the DFT method for the proton-transfer reactions. The reaction energies for the combined protonation and O–O bond cleavage for Cpd 0 bearing anionic proximal ligands (**6a,c,e**) are listed in Table 2 that also gives in parentheses those corrected for harmonic zero-point energy (ZPE) contributions.

With formic acid (pK<sub>a</sub> 3.8), the O–O bond cleavage is essentially isoenergetic for catalase model **6e** (non-ZPE-corrected), while this reaction is less favorable for the P450 (**6a**) and peroxidase (**6c**) models by as much as 4.5 and 10.7 kcal mol<sup>-1</sup>, respectively. By including ZPE corrections the dissociation energies reduce by 3.3–4.8 kcal mol<sup>-1</sup>, making that for the catalase model modestly exothermic and that for the P450 model nearly isoenergetic. Decreasing the acid strength of the proton source (pK<sub>a</sub> 3.6 → 17.1) increases the endothermicity for each system by about 30 kcal mol<sup>-1</sup>. Thus, the proton assisted O–O bond cleavage appears feasible at modest acidities, having different rates that depend on the proximal ligand. This is in accord with the experimental observation that histidine coordinated porphyrins are able to catalyze P450 type oxygen transfers and that cysteine coordinated porphyrins can catalyze peroxidase type reactions.<sup>39–44</sup> It is important to emphasize, however, that the formation of Cpd I is modestly endothermic for the P450 model bearing a proximal thiolate ligand (**6a**) irrespective of the proton donor source. This finding relates to recent QM and QM/MM studies that reported similar energies for Cpd 0 and I, taking charge balancing into account,<sup>11,24b</sup> and that suggested the presence of a barrier for the Cpd 0 → I conversion.<sup>11,25a</sup>

Comparing the two model reactions 1 and 2 with each other using the same proton donor, i.e., β-alanine (pK<sub>a</sub> 3.6) and its conjugate acid β-alanine-H<sup>+</sup> (Tables 2 and 3), shows that protonating the proximal ligands facilitates the O–O bond cleavage of the Cpd 0 P450 (**6a** vs **6b**) and catalase (**6e** vs **6f**) models, be it with only a very modest 3.5 and 3.2 kcal mol<sup>-1</sup>, respectively.<sup>45</sup>

In contrast, the effect is rather substantial on protonating the imidazolate ligand of the peroxidase model (**6c** vs **6d**), changing an endothermic O–O bond cleavage (ΔE 12.0 kcal mol<sup>-1</sup>) to an exothermic one (-3.4 kcal mol<sup>-1</sup>). These calculations are in accord with the current view of heme proteins where the

- (39) Blanke, S. R.; Hager, L. P. *J. Biol. Chem.* **1988**, *263*, 18739–18743.  
 (40) Sundaramoorthy, M.; Temer, J.; Poulos, T. L. *Structure* **1995**, *3*, 1367–1377.  
 (41) Fraaije, M. W.; Roubroeks, H. P.; Hagen, W. R.; Van Berkel, J. H. *Eur. J. Biochem.* **1996**, *235*, 192–198.  
 (42) Rusvai, E.; Vegh, M.; Kramer, M.; Horvath, I. *Biochem. Pharmacol.* **1988**, *37*, 4574–4577.  
 (43) Nakamura, S.; Mashino, T.; Hirobe, M. *Tetrahedron Lett.* **1992**, *33*, 5409–5412.  
 (44) Osman, A. M.; Koerts, J.; Boersma, M. G.; Boeren, S.; Veeger, C.; Rietjens, I. M. C. M. *Eur. J. Biochem.* **1996**, *240*, 232–238.  
 (45) This is interpretation differs from the mechanistic “push effect” (Dawson, J. H. *Science* **1988**, *240*, 433–439; Poulos, T. L. *Adv. Inorg. Biochem.* **1987**, *7*, 1–52) in which the anionic thiolate ligand serves as a strong electron donor to facilitate the heterolytic O–O bond cleavage in the catalysis of the natural P450 enzymes. However, more recently, this effect has been considered to have only a relatively minor influence (Poulos, T. L. *J. Biol. Inorg. Chem.* **1996**, *1*, 356–359).

**Table 4.** Reaction Energies (kcal·mol<sup>-1</sup>) for the Proximal Protonation of Cpd 0 by Zwitterion 3-Aminopropanoic Acid ( $n = 0$ ) and 3-Ammoniopropanoic Acid ( $n = 1$ ) Generating the Hydrogenperoxide Complex

$$\begin{array}{c} \text{O} \\ | \\ \text{O}-\text{O}-\text{H}^{\ominus n-1} \\ | \\ \text{Fe} \\ | \\ \text{(H)X} \end{array} + \text{AH}^n \longrightarrow \begin{array}{c} \text{H} \\ | \\ \text{H}-\text{O}-\text{O}-\text{H}^{\ominus n} \\ | \\ \text{Fe} \\ | \\ \text{(H)X} \end{array} + \text{A}^{n-1} \quad (3)$$

	(H)X		
	(P450) H <sub>n+1</sub> S	(peroxidase) ImH <sub>n</sub>	(catalase) MePhOH <sub>n</sub> <sup>a</sup>
$n = 0$	+24.4	+34.6	+30.5
$n = 1$	+30.9	+21.4	[+35.6]

<sup>a</sup> For  $n = 1$ , 4-methyl phenolate coordinated to a methylguanidinium cation has been used, as a mimic for the conserved arginine in catalases.

presence of an uncharged histidine amino acid is assumed in peroxidases and a neutral arginine/tyrosine pair in catalases.<sup>20,37</sup> These uncharged proximal regions facilitate the formation of the experimentally detected Cpd I. For cytochromes P450, which have a negatively charged proximal cysteine ligand, this is not the case, which could suggest that it is the protonation of the axial ligand that influences the chemistry of Cpd 0 rather than the nature of the ligand.

As the DFT calculations show that the heterolytic cleavage of the O–O bond of the three models can be endothermic, it becomes relevant to evaluate this path for **6a–f** against that of protonating the proximal (inner) oxygen of Cpd 0. Namely, the so-called peroxide shunt mechanism is initiated by the hydrogen peroxide complex that ultimately results in the unwanted consumption of the oxidant O<sub>2</sub> without substrate oxidation. The energies of protonating the proximal oxygen of Cpd 0, carrying an ionic or neutral ligand (**6a–f**), and using  $\beta$ -alanine as the moderate proton source are listed in Table 4 (eq 3). The data clearly show the formation of the hydrogen peroxide complex to be highly endothermic (21–35 kcal mol<sup>-1</sup>). In fact, this path is disfavored from protonation of the distal oxygen atom that leads to Cpd I, by as much as 19–38 kcal mol<sup>-1</sup> when using  $\beta$ -alanine as a proton source. Consequently, we assume that the distal oxygen atom is protonated first.

In contrast to the extensive theoretical work that has been performed on P450 models, the corresponding formation of Cpd I from the peroxidase and catalase models has hardly been addressed. However, we note that our peroxidase model reaction 2 agrees with a study in which an imidazole moiety was used to protonate the outer oxygen atom of an imidazole ligated iron hydroperoxo model with concomitant O–O bond cleavage.<sup>46</sup> In this study the porphyrin was replaced by two [(NH)(CH<sub>3</sub>)(NH)]<sup>-</sup> groups.

So far, we have seen that the formation of Cpd I is endothermic at OPBE/TZP for the P450 models. This is also the case when the protein environment of P450cam is included. We established this using our QM/MM approach (Figure 1 and Supporting Information) with glutamic acid (Glu366) acting as a proton donor via a H-bonded network of water molecules.<sup>5a</sup> In fact, the calculated energy difference of 7.7 kcal mol<sup>-1</sup> between the fully optimized Cpd 0 and I is remarkably similar to that obtained at DFT using moderate acids as proton sources.

(46) Wirstam, M.; Blomberg, M. R. A.; Siegbahn, P. E. M. *J. Am. Chem. Soc.* **1999**, *121*, 10178–10185.

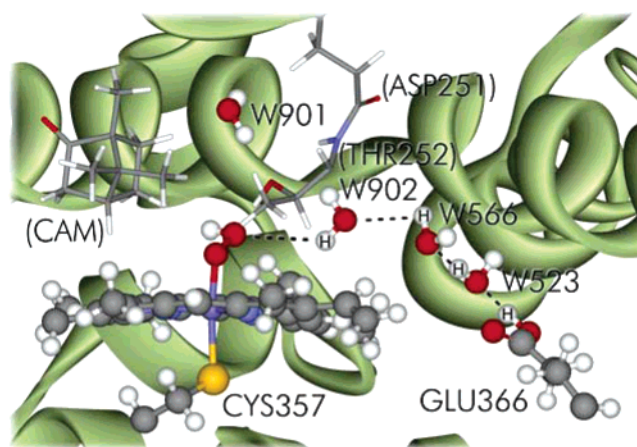


**Figure 1.** QM/MM-optimized geometry for Cpd 0 showing the glutamic acid as a proton source and the water molecules (W523, W566, W901) acting as the proton-transfer network in the formation of Cpd I (optimized QM/MM geometry in the Supporting Information). The atoms included in the QM(DFT(OPBE/TZP)) part are displayed as balls-and-sticks, and the atoms in the MM(amber) part are displayed as sticks. The labels of the MM residues are given in parentheses. The energy difference between Cpd I and Cpd 0 is 7.7 kcal mol<sup>-1</sup>.

However, a note of caution is necessary as we found the relative energy to be sensitive to small perturbations in the QM/MM setup (i.e., starting structure). Similar observations were made by the groups of Shaik and Thiel, who studied the protonation machinery with B3LYP/CHARMM.<sup>47</sup> However, these authors found the chain of water molecules to be broken by the alcohol group of Thr252 indicating the dynamic character of the assembly, which warrants a more thorough investigation in the future.<sup>48</sup>

Next we investigate the Cpd 0 → I process in more detail at DFT. Because of the complexity of locating transition structures for large systems containing several water molecules and amino acid residues, we used the thiolate iron porphyrin hydroperoxide model with the noted three acids as mimics for the amino acids present in the active sites of heme containing oxidoreductases. The Cpd 0 → I conversion can be mapped by varying (1) the O–O distance of the OOH<sup>-</sup> group and (2) the AH–O distance between the outer oxygen atom of Cpd 0 and the proton of the acid (AH), for which the moderate imidazole, the strong formic acid, and the weak isopropyl alcohol are used to mimic the distal proton delivery. We include imidazole in our evaluation even though histidine is not present in the P450 active site, for reasons of consistency with the earlier part of this study and for providing insight into the dependency of the acidity on the reaction barrier.

The potential energy surface (PES), shown in Figure 2A, gives a +11.7 kcal mol<sup>-1</sup> barrier for the imidazole assisted heterolytic O–O bond cleavage (Figure 2B);<sup>49</sup> this result contrasts with the notion that the formation of Cpd I occurs without a barrier<sup>2,3,25</sup> but substantiates the recently suggested barrier based on constrained geometry optimizations.<sup>11</sup> The

(47) Zheng, J.; Wang, D.; Thiel, W.; Shaik, S. *J. Am. Chem. Soc.* **2006**, *128*, 13204–13215.

(48) One of the referees stressed the importance of this hydrogen bridged Thr252 because it hampers or even prevents protonation at an earlier stage of the catalytic cycle, i.e., structure 4 (Scheme 1).

(49) To account for spin contamination in the doublet transition states (<sup>S2</sup> TS1: 1.13; TS2: 0.93) and Compound I (1.27), a correction based on the expected value of <sup>S2</sup> calculated over the Kohn–Sham determinants is used, as described in ref 31.

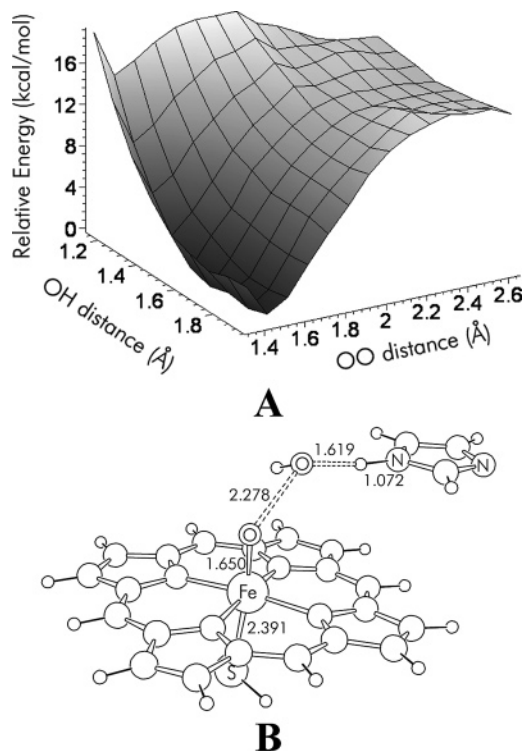


**Figure 2.** (A) Potential energy surface (doublet) for formation of Compound I as a function of the O–O and O–H bond distances with imidazole as a proton donor. (B) The optimized OPBE/TZP transition structure for formation of Cpd I by protonation of Cpd 0 with imidazole (distances in Å).

optimized transition structure, depicted in Figure 2B, has an imaginary frequency of  $121i\text{ cm}^{-1}$  that reflects the O–O stretching mode. Increasing the O–O distance leads to a ca.  $2\text{ kcal mol}^{-1}$  lower plateau for several isoenergetic structural combinations of Cpd I, water, and the imidazololate anion. Using formic acid and isopropyl alcohol as proton sources gives barriers for the O–O scission of  $+7.8$  and  $+12.2\text{ kcal mol}^{-1}$ , respectively. On including the ZPE corrections these barriers reduce by  $2.2\text{--}3.1\text{ kcal mol}^{-1}$ , which we presume to be an upper limit due to the harmonic approximation. The corresponding optimized transition structures have imaginary frequencies of  $130i\text{ cm}^{-1}$  and  $146i\text{ cm}^{-1}$ . Also for these acids a smooth potential energy surface is reached on further stretching of the O–O bond. Cpd I formation in the presence of isopropanol can best be described as an acid-assisted O–O bond elongation. Increasing the acidity with imidazole gives essentially the same picture, whereas further decrease of the  $pK_a$  (formic acid) gives O–O bond scission with concurrent protonation. This behavior is also reflected in the transition structures with that of formic acid showing a shorter O–H and a longer H–A bond distance and isopropanol showing relatively long O–H and short H–A bond distances (Table 5).

In conclusion, the acidity of the distal heme region influences significantly the proton assisted formation of Cpd I. As expected,

**Table 5.** Selected Bond Distances (Å), Activation Energies (EA), and ZPE Corrected Energies in Parentheses ( $\text{kcal mol}^{-1}$ ) for the Proton Assisted O–O Bond Cleavage of Model P450 Cpd 0 (doublet)

acid AH	bond distances (Å)				EA ( $\text{kcal mol}^{-1}$ )
	Fe–O	O–O	O–H	H–A	
imidazole <b>TS1</b>	1.650	2.278	1.619	1.072	+11.7 (+9.2)
formic acid <b>TS2</b>	1.636	2.235	1.075	1.398	+7.8 (+4.7)
isopropanol <b>TS3</b>	1.651	2.339	1.690	1.006	+12.2 (+10.0)

lowering the  $pK_a$  of the proton source decreases the endothermicity of the reaction. The manner by which the proximal heme ligand of Cpd 0 is protonated is an important regulatory component in the catalytic cycle of heme containing oxidoreductases. Protonation of the proximal Cpd 0 ligand favors distal heterolytic O–O bond scission. The Cpd 0  $\rightarrow$  I conversion for cytochromes P450 is endothermic and has a sizable barrier with the magnitude depending on the strength of the proton donor, while the Cpd I  $\rightarrow$  0 back reaction has a very small barrier of ca.  $2\text{ kcal mol}^{-1}$ . This result is in agreement with Cpd 0 being the last observable reaction intermediate in the catalytic cycle of the P450s. A slightly exothermic Cpd 0  $\rightarrow$  I conversion is estimated for the peroxidases and catalases for which Cpd I has been observed experimentally. These calculations demonstrate that the nature of the proton delivery channel is critically important in the energetic relationship between Cpd 0 and I. For the P450s this could imply that conversion(s) of Cpd 0 to potential oxidants other than Cpd I may have to be considered in light of, for example, the reported barrier for the homolytic O–O bond cleavage (ranging from  $19.4$  to  $24.8\text{ kcal mol}^{-1}$ )<sup>12</sup> and that for the alkane H-abstraction by Cpd I (ranging from  $14.0$  to  $28.6\text{ kcal mol}^{-1}$ ).<sup>7,16</sup> Carefully calibrated QM/MM studies on the influence of the protein environment on the reaction energies and barriers for such potentially competing/complementary alkane oxidations starting from Cpd 0 are needed and are being performed by us to obtain a more comprehensive mechanistic understanding.

**Acknowledgment.** Dr. M. Swart is acknowledged for providing the AddRemove coupling scheme prior to the official release of ADF. The Center of Complex Molecules of the Vrije Universiteit is acknowledged for financial support and the National Computing Facilities Foundation (NCF) for the use of their supercomputer facilities with financial support from the Netherlands Organization for Scientific Research (NWO). We also want to thank the referees for their critical, yet constructive comments.

**Supporting Information Available:** Additional computational details, gas-phase proton affinities, Cartesian coordinates, energies, and tables with key optimized geometries together with selected bond distances, charges, and spin densities. This material is available free of charge via the Internet at <http://pubs.acs.org>.

JA0685654